1

Convective mixing and high littoral production established systematic errors in the

diel oxygen curves of a shallow, eutrophic lake

Soren Brothers[a,*], Garabet Kazanjian, Jan Köhler, Ulrike Scharfenberger, Sabine Hilt

Leibniz-Institute of Freshwater Ecology and Inland Fisheries, Berlin, Germany

[a] Present Affiliation: School of Environmental Sciences, University of Guelph, Guelph,

Ontario, Canada

[*] Corresponding author: Soren Brothers (sbrother@uoguelph.ca)

School of Environmental Sciences, University of Guelph

Bovey Building, Gordon St.

Guelph, Ontario, N1G 2H1

Canada

Running Head: Diel oxygen curves method reassessment

24   **Abstract**

25   The diel (24-hour) oxygen (O_2) curves approach has become a popular method for

26   analyzing gross primary production (GPP) and ecosystem respiration (ER) rates in

27   aquatic systems. Despite the simplicity of this approach, there remain aspects of the

28   calculation and interpretation of diel O_2 curves which may skew results, with potentially

29   large implications for estimates of metabolic rates. One common problem in lakes is the

30   occurrence of unexpected changes in O_2 concentrations (for instance, increasing

31   overnight O_2 concentrations). Such changes have typically been ascribed to the random

32   mixing of pockets of O_2. It has thus been suggested that negative GPP or positive ER

33   values should be included in calculations, on the assumption that under- and

34   overestimates should occur with equal frequency, and thus cancel each other out. Our

35   data from a shallow, eutrophic lake provided a high share of negative GPP values. We

36   argue that these may have been the result of elevated littoral productivity coupled with

37   convective currents produced by consistent differences in the heating or cooling of littoral

38   and offshore waters. Such phenomena might be common in small, sheltered lakes where

39   the role of mixing by wind is diminished. We conclude that a failure to account for

40   consistent metabolic gradients and periodic convective mixing may lead to a chronic

41   underestimation of metabolic rates in lakes when using the diel O_2 curves method.

42

43

44

45

46

Introduction

The diel (24-hour) oxygen (O_2) curve technique has rapidly become an accepted standard approach for measuring metabolic rates in aquatic ecosystems since being designed for fluvial systems six decades ago (Odum, 1956). By measuring the rates at which pelagic day- and nighttime O_2 concentrations change, this approach offers researchers an elegant, simple way to quantify ecosystem respiration (ER) and gross primary production (GPP) rates (Staehr et al., 2010; Hoellein et al., 2013). Specifically, Hanson et al. (2008), adapting from Odum (1956), proposed that the areal rate of change of dissolved oxygen (Q) at a given station could be calculated using the model:

$$Q = GPP - R + D + A \qquad (1)$$

Where GPP is the areal rate of gross primary production, R is the areal community respiration rate, D is the local flux of O_2 between the water surface and atmosphere, and A represents all other O_2 fluxes, such as those resulting from vertical or horizontal mixing. For rapidly-and thoroughly-mixed fluvial systems, diel O_2 curves based on single probe deployments are expected to represent both benthic and water column production. In lakes, the degree to which whole-lake metabolic rates can be accurately estimated using the diel O_2 curves method varies with the location and duration of an O_2 probe's installation, the rate at which a lake's water column is mixed, and the metabolic variability within a given mixed layer (Van de Bogert et al., 2012; Obrador et al., 2014). Calculated GPP values might therefore only represent phytoplankton production rates within the measured mixed layer, and the degree of benthic and littoral periphyton (attached algae) or macrophyte contribution would increase with water mixing and/or measuring proximity to those environments (Coloso et al., 2008). Considering the

70   potentially large variations in metabolic rates between the water column, benthos, and

71   littoral zones of a given lake, the chosen measurement location may influence the

72   resulting data (Lauster et al. 2006; Caraco and Cole 2002; Van de Bogert et al., 2007;

73   Sadro et al., 2011; Staehr et al., 2012). Littoral macrophyte beds can boost net ecosystem

74   production (NEP), producing high dissolved O_2 concentrations in the littoral surface

75   waters compared to offshore surface waters (Unmuth et al., 2000; Lauster et al., 2006;

76   They et al., 2013; Idrizaj et al. 2016; Fig. 1).

77   With rapid and/or random mixing of lake waters, elevated littoral primary

78   productivity rates might influence long-term offshore O_2 curves. However, during low-

79   wind periods or sheltered conditions, convective currents created by differences in

80   nighttime cooling or daytime heating rates between the shallow littoral zone and deeper

81   offshore zone may come to dominate lake circulation patterns (Horsch and Stefan, 1988;

82   MacIntyre and Melack, 1995; Forrest et al., 2008; Fig. 1). Such convective forces may

83   produce both horizontal and vertical penetrative currents, and are usually associated with

84   the summer and winter months (Forrest et al., 2008; Salonen et al., 2014). Summertime

85   littoral-to-offshore flow rates have been measured from 4 to 20 m h^{-1} (James and Barko,

86   1991), while littoral flushing periods have been estimated of one to four hours, varying

87   with macrophyte cover (Oldham and Sturman, 2001). The regular occurrence of such

88   convective currents, coupled with typically elevated daytime O_2 production in the littoral

89   zone (relative to the off-shore water column), could feasibly result in a nightly recurrent

90   bias whereby nighttime O_2 concentrations increase at off-shore sites in lakes, producing

91   negative metabolic values (Fig. 2). Similarly, elevated littoral O_2 depletion at night could

92   result in a supply of O_2-depleted water to the lake center the following day, with the same

93   outcome for calculated metabolic rates (Fig. 2). Such impossible negative GPP values

94   have been reported when applying this method to lakes, though it has been suggested that

95   they are likely the result of the random mixing of pockets of high and low dissolved O_2 in

96   the water column, or term "A" in Eq. 1 (Staehr et al., 2010). It has therefore been

97   assumed that underestimated values, which we here consider to be (metabolically

98   impossible) negative GPP values calculated from low daytime NEP or positive calculated

99   ER rates (i.e. oxygen concentrations increasing overnight absent primary production),

100   occur as frequently as overestimated values, with the suggested solution being that all

101   values be included in the calculations of mean metabolic rates (Staehr et al., 2010).

102   In this study, we analyzed diel O_2 curves and concurrent independent

103   phytoplankton GPP measurements from a small, shallow temperate lake to examine the

104   frequency, seasonality, and severity of GPP rates that were calculated to be negative. We

105   predicted that convective mixing coupled with higher littoral GPP may introduce a

106   systematic bias into our estimated metabolic rates. Such bias could be especially

107   significant when applying the diel O_2 curve method to embayments or small, sheltered

108   lakes with high littoral-to-pelagic ratios, where convective mixing may play a large role.

109   A re-evaluation of the applicability of the diel O_2 curves method for metabolic rates in

110   small lakes could have broader implications for global estimates of metabolism in aquatic

111   ecosystems. New research has documented that lakes play an important role in regional

112   and global carbon cycling (Tranvik et al., 2009). Furthermore, most lakes have surface

113   areas less than 1 km^2 and are often characterized by a high percentage of lake area

114   occupied by the littoral zone, and possibly a high degree of sheltering from wind (for

115   instance, by surrounding trees), and thus present a greater potential role for convective

116   mixing (Downing et al., 2006; Verpoorter et al., 2014). It is thus important to determine

117   whether such a bias exists, and to quantify how severe it might be.

118

119   **Materials and procedures**

120   We present data from Schulzensee (53°14'N, 13°16'E), a small (3 ha, radius = ~

121   100 m), shallow, eutrophic lake (mean total phosphorus concentration in 2010: 34 ± 3 µg

122   L^{-1}) located in a rural lowland area of northeastern Germany. Schulzensee's primary

123   production is provided by phytoplankton and periphyton, non-rooted submerged

124   macrophytes (primarily *Ceratophyllum submersum*) in the littoral areas during

125   summertime, and colony-forming benthic cyanobacteria (*Aphanothece stagnina*)

126   (Brothers et al., 2013a,b). Though fed by groundwater, this lake features no surface

127   inflows or outflows, and is naturally sheltered by alder trees (*Alnus glutinosa*) and located

128   in a forested depression. It is thus expected to experience only minor wind-driven

129   resuspension. Schulzensee's littoral zone occupies roughly 32% of the lake surface area,

130   and its shallow mean depth (2.2 m) resulted in a relatively large proportion (~50%) of the

131   whole-lake GPP being represented by benthic production (Brothers et al., 2013b).

132   Yellow Springs Instruments (YSI, Xylem Inc., Yellow Springs, OH, USA) sondes

133   were installed at a lake-center monitoring station from May 8th, 2010 to May 7th, 2011, at

134   a depth of approximately 1.2 m (varying with minor lake level fluxes). These sondes

135   recorded temperature, O_2, and pH every 10 minutes during the full year. YSI sondes were

136   also used to measure vertical profiles from the surface to sediments (at gradients of 0.5

137   m) every four weeks throughout the study period. GPP and ER were calculated from diel

138   O_2 curves (Eq. 1) following the procedures of Staehr et al. (2010), also known as the

139 "bookkeeping approach". Specifically, ER was calculated as the mean change in O_2 (per

140 10 minutes) from one hour after dusk until dawn (thus typically giving it a negative sign).

141 ER was subtracted from net production (NP) rates calculated by the same methods for the

142 following day to provide GPP (typically giving it a positive sign). Diel O_2 curves were

143 corrected for atmospheric O_2 fluxes following Gelda and Effler (2002), using lake-center

144 wind speed data recorded every 10 minutes by a meteo multiprobe (ecoTech, Bonn,

145 Germany). Surface fluxes were corrected for a period of stratification (July 16th to August

146 24th) by adopting the mean measured surface O_2 concentrations from profiles to avoid

147 overestimating O_2 losses to the atmosphere. Production values are expressed in carbon

148 units applying a respiratory quotient of one. Although the fundamental assumptions of

149 our hypothesis may be considered applicable to both GPP and ER values (Fig. 1), our

150 analyses focus on calculated GPP values, since GPP was the metabolic parameter for

151 which corollary data (as phytoplankton GPP) were available. Convective mixing is

152 expected to affect daytime O_2 curves as well as nighttime ones (Fig. 1), though we here

153 focus on the phenomenon of increasing nighttime O_2 curves, which cannot be explained

154 by metabolic processes. Since daytime net production is influenced by both GPP and ER

155 concomitantly, it can feasibly be positive or negative, making the non-metabolic effects

156 of mixing on daytime curves more difficult to identify.

157   Independent calculations of pelagic (lake-center) phytoplankton GPP were made

158 from monthly measurements of chlorophyll *a* (Chl *a*) concentrations (mixed depth lake-

159 center samples, from 0.5 m, 1 m, and 2 m), fluorescence, and light attenuation (Brothers

160 et al., 2013b). Photosynthetic parameters were obtained from rapid photosynthesis-

161 irradiance (P-I) curves measured within three hours of sampling using the modular

162   version of a Phyto-PAM fluorometer (Phyto-PAM, Walz, Effeltrich, Germany) equipped

163   with a 10 mm cuvette. The concentration of Chl a in water samples was measured by

164   high-performance liquid chromatography (HPLC, Waters, Millford, MA, USA),

165   following Shatwell et al. (2012). Phytoplankton GPP was calculated for each 10 cm layer

166   of the water column using hourly depth-specific PAR (derived from global radiation at

167   the water surface and light attenuation of the water column), with each measurement

168   being multiplied by the estimated water volume at a specific depth. The sum of these

169   measurements was used to calculate daily whole-lake phytoplankton production

170   (Brothers et al., 2013b). Due to an anticipated minimal light transmission through heavy

171   snow and ice, phytoplankton GPP could not be reliably calculated, and was thus assumed

172   to be zero during the full period of ice cover (December 1st, 2010 to March 15th, 2011).

173   Statistical tests were made using JMP (Version 7, SAS Institute) and values are provided

174   with standard error of the mean unless otherwise specified.

175

176   **Assessment**

177   Over the course of the full study year, O_2 curves from 293 24-hour periods were

178   available for analysis. This was after accounting for sonde malfunction and two outliers,

179   which occurred during periods of potential ice break-up, during which lake surface-to-

180   atmosphere O_2 flux rates could not be established. The mean GPP rate calculated by the

181   diel O_2 curve method with negative values included (following the standard book-

182   keeping approach) was 83 ± 21 g C m^{-2} y^{-1}. When negative values were excluded, the

183   full-year mean value rose significantly to 315 ± 22 g C m^{-2} y^{-1} (Wilcoxon Test, $p <$

184   0.0001). Independently determined phytoplankton GPP rates calculated from

185   fluorescence measurements for the same dates as available O_2 curves were 216 ± 12 g C

186    $m^{-2} y^{-1}$ (Table 1).

187   The significant difference between GPP calculations with and without the

188   inclusion of negative values results from the abundance of such abnormal values.

189   Increasing nighttime O_2 concentrations were observed on 45% of the available dates

190   (Table 1, Fig. 3). Seasonally, these were found to occur most frequently in winter

191   (December to February; 81%), followed by summer (June to August; 40%), fall (March

192   to May; 32%) and spring (September to November; 30%). The exclusion of negative GPP

193   values significantly affected the mean calculated values for all seasons in this lake ($p <$

194   0.05, Wilcoxon Test). The severity of this effect was greatest in summer and winter

195   months (Table 1), the summer influencing annual GPP mean values to a greater extent

196   due to their lower values (minimum GPP = -2802 mg C $m^{-2} d^{-1}$) compared to those in the

197   winter (minimum GPP = -742 mg C $m^{-2} d^{-1}$).

198

199   **Discussion**

200   When inaccuracies in daily GPP estimates result from measurement imprecision

201   or random patterns of O_2 dispersion in the water column of a lake, underestimates and

202   overestimates in GPP rates should balance each other out, providing accurate mean

203   productivity rates over time. Based on this assumption, standard procedures suggest the

204   inclusion of negative GPP estimates and lengthy sampling periods (e.g., Staehr et al.,

205   2010). In our study lake the inclusion of negative GPP values would provide roughly four

206   times lower annual GPP rates than with negative values excluded. A comparison of these

207   values with mean phytoplankton GPP over the same sampling dates (216 ± 12 g C $m^{-2} y^{-}$

208   [1]) indicates that the inclusion of negative GPP values in the O_2 curves approach

209   (providing a mean of 83 ± 21 g C m^{-2} y^{-1}) is not balanced out by overestimation, and thus

210   the inclusion or exclusion of negative values leads to a systematic bias, and likely

211   introduces inaccuracies. Furthermore, the inclusion of the negative GPP values not only

212   underestimates phytoplankton GPP in this lake, but it also fails to capture any additional

213   littoral periphyton production occurring within the mixed layer. This is corroborated by a

214   regression from del Giorgio and Peters (1993), linking pelagic Chl a concentrations to

215   phytoplankton GPP calculated via the same methodology. Given a mean annual Chl a

216   concentration of 13 µg L^{-1} (from Brothers et al., 2013a), pelagic phytoplankton GPP in

217   our study lake should be approximately 175 g C m^{-2} y^{-1} (assuming a mean lake depth of

218   2.2 m).

219   For convective mixing to be the source of our observed bias, littoral oxygen

220   concentrations would need to be higher than pelagic oxygen concentrations (in order to

221   increase nighttime lake-center oxygen concentrations), and convective currents would

222   need to flow at a rate sufficient to transport water from the littoral zone to the lake center

223   within a nighttime period. The YSI sonde in our study lake was situated approximately

224   80 m from the nearest littoral zone, meaning that a flow rate of roughly 7 m h^{-1} would be

225   required for midday O_2-rich littoral waters to travel convectively to reach the probe by

226   midnight. This flow rate is well within the range of convective flow rates (4 to 20 m h^{-1})

227   described by James and Barko (1991). As part of a separate, later analysis, YSI sondes

228   (of the same model as that in our study, and both with 10-minute sampling frequencies)

229   measured littoral and pelagic O_2 concentrations simultaneously in this lake during a two-

230   week period in September 2011. They confirmed that mean O_2 concentrations were

231   significantly higher in the littoral zone (2.66 ± 0.03 mg L^{-1} n = 2160) than in the pelagic

232   zone (1.49 ± 0.03 mg L^{-1}; n = 2087; Wilcoxon Test, $p < 0.0001$). We do not have enough

233   data to say whether this difference between habitats was a result of net metabolic

234   differences, differing rates of aeration due to wave action in the shallower depths of the

235   littoral, or the result of a somewhat shallower probe exposure depth (~0.5 m) in the

236   littoral zone compared to the pelagic probe (~0.8 m during this later study period).

237   Forrest et al. (2008) note that summer and winter months, when shear stresses due to

238   wind have their lowest effects on temperate lakes, are the periods when convective

239   mixing plays the largest role. Notably, these were also the seasons during which our

240   study lake, as well as another similarly-sized lake in the region for which O_2 curves were

241   available (data not shown), experienced the highest frequency and strongest effect of

242   false negative GPP rates. Ice covered our study lake during the full winter period, while

243   the summer months featured the largest daily difference in air temperatures, as well as the

244   lowest wind speeds, making both seasons ideal for maximizing the effects of convective

245   mixing events on O_2 concentrations (Table 1). However, to definitively conclude that

246   convective mixing was the source of false negative GPP rates would require detailed

247   measurements of water flow rates, as well as littoral and pelagic O_2 concentrations.

248   False negative GPP rates can also be a result of other physical factors. Daily

249   microstratification dynamics, producing deeper mixing depths in the morning and

250   shallower ones in the afternoon (Coloso et al., 2011), could potentially result in periodic

251   errors if YSI sondes cross periodically between mixing zones. Although profiles revealed

252   summertime vertical O_2 concentration gradients in this lake, estimated mixing depths

253   during our study period were typically greater than 1.5 m depth (data not shown). These

254 estimates were derived from data typically collected around midday or the early

255 afternoon, suggesting that it is feasible that mixing depths in the late afternoon may be

256 lower (Coloso et al., 2011), producing sudden shifts in measured O_2 concentrations.

257 However, Tinytag temperature loggers (Gemini Data Loggers Inc, Chichester, UK)

258 installed at every 50cm depth following our study period (July 29th to October 14th, 2011)

259 detected no notable (>0.25 °C), recurrent daily shifts in temperature between one and two

260 meters below the surface, where our sonde had been located.

261   We furthermore considered the possibility that oxygen-poor groundwater entering

262 the lake may have influenced the measured diel O_2 curves. Groundwater volumetric

263 fluxes had been estimated for this lake during the same period using data taken from two

264 small wells in the immediate vicinity (four to six meters from the shore). Given the lack

265 of surface inflows or outflows to this system, monthly groundwater fluxes were

266 occasionally large, representing as much as ~6% of the full lake water volume (data not

267 shown), potentially decreasing summertime O_2 concentrations by that same fraction

268 (assuming groundwater to be anoxic). However, groundwater loading would not fluctuate

269 along a daily, periodic cycle, and thus would not be expected to influence diel O_2 curves

270 measured over a prolonged exposure period.

271   The total GPP of Schulzensee during this study year (including benthic, littoral,

272 and pelagic primary producers) was estimated by Brothers et al. (2013b) to be 550 g C m[-]

273 [2] y[-1] (one third of which was attributed to phytoplankton). It is thus feasible that positive-

274 only O_2 curve GPP rates (315 ± 22 g C m^{-2} y[-1]) provided a roughly accurate estimate of

275 mixed-layer GPP alone, assuming that benthic GPP may not have been fully mixed into

276 the surface water layer. However, as one may still anticipate false positives and false low

277 GPP values (even if they are not negative), we cannot suggest that the automatic

278 exclusion of negative GPP values will provide reliable data. Rather, the amplitude of the

279 bias from convective mixing would vary according to factors such as seasonality, plant

280 community structure, wind exposure, lake fetch and bathymetry, and O_2 probe placement.

281   We suggest that, in addition to random mixing events, periodic mixing events

282 such as convective mixing could play a major role in the physical mixing of O_2 in small

283 lakes, which could in turn negatively affect diel O_2 curve calculations. On a small-to-

284 medium timescale (days to weeks), rapid and variable changes in O_2 concentrations could

285 result from random processes such as wind-driven mixing (e.g., Cremona et al., 2014).

286 Such occurrences may be treated using "smoothing" modeling approaches (designed to

287 reduce variability), such as Bayesian models (Solomon et al., 2013; Cremona et al., 2014)

288 or Kalman filters (Batt and Carpenter, 2012). A separate analysis of our dataset using

289 multiple modeling approaches (Bayesian, bookkeeping, Kalman, maximum-likelihood

290 estimation, and ordinary least squares) provided by the R package "LakeMetabolizer"

291 (Winslow et al., 2016) reveals that the smoothing models are successful at constraining

292 the range of GPP values produced, but the overall mean GPP values do not differ

293 significantly between approaches (Wilcoxon Test, $p = 0.94$) and negative GPP values

294 remain common (Fig. 4).

295   Random mixing events (here considered any which do not occur on a regular 24-h

296 cycle) typically occur in the spring and fall, when the water column is frequently mixed

297 by low vertical temperature-driven density gradients and higher winds. However, diel

298 periodic mixing patterns are most likely to establish during summer and winter, when the

299 effects of wind on water column mixing are reduced, especially in lakes in landscape

300   depressions sheltered from the wind. Due to the periodicity of such events, models which

301   simply reduce the mixing weight (i.e. relative calculated importance) of outliers or highly

302   variable events are poorly suited to derive reliable metabolism rates during such periods.

303   Adding complexity to diel O_2 calculations also fails to enhance the accuracy of metabolic

304   calculations when processes such as internal waves, microstratification, or convective

305   currents influence the variability of O_2 in the water column (Hanson et al., 2008). We

306   therefore propose that an enhancement to Odum's (1956) fundamental calculation of diel

307   O_2 curves is needed, especially when considering small, sheltered lakes:

308   $$Q = GPP - R + D + A_r + A_p \quad + GW \qquad\qquad (2)$$

309   The term "GW" has been introduced to reflect the possible role played by anoxic

310   groundwater intrusion on small lakes lacking surface in- or out-flows. The term "A",

311   which initially represented water column mixing (Eq. 1), is here divided into "A_r",

312   representing random mixing events (e.g., wind-driven mixing), and "A_p," representing

313   periodic mixing events such as convective mixing following different warming/cooling

314   regimes between nearshore and offshore waters, or daily microstratification events.

315   During spring and fall, A_r is anticipated to play an important role, and the use of

316   smoothing models such as Kalman filters (Batt and Carpenter, 2012), or the removal of

317   dates with high wind speeds or low solar irradiance (Rose et al., 2014) is recommended

318   to reduce the presence of outliers. While the effect of A_p on diel O_2 curves may be

319   greatest in summer and winter, its magnitude depends upon lake size and bathymetry,

320   changes in air temperature, and the difference between littoral and off-shore O_2

321   production, making it more difficult to predict.

322

323 **Comments and recommendations**

324   Although diel O_2 curves remain one of the most cost- and time-efficient methods

325 for calculating metabolic rates in aquatic ecosystems, we note that their utility may be

326 limited in some situations. We advise researchers to critically examine the frequency and

327 severity of false negative metabolic rates, taking into consideration possible factors which

328 could be responsible for producing them, especially if they comprise a significant share

329 of calculated rates. Although it is possible to estimate horizontal exchange flow rates

330 based on the littoral benthic slope (e.g., Sturman et al., 1999), more research (including

331 direct measurements with an acoustic Doppler current profiler) would be necessary to

332 establish whether such a calculation could provide enough information to reliably avoid

333 the common recurrence of false negative metabolic values. As a first step, we suggest that

334 researchers adopt multiple independent approaches when determining ecosystem

335 productivity. Additionally, in lakes in which periodic mixing events (A_p in Eq. 2) such as

336 convective mixing or microstratification events may occur (during summer or wintertime

337 months in shallow lakes or embayments), multiple sampling depths and distances from

338 the littoral zone during these seasons may improve the reliability of metabolism rates

339 calculated from diel O_2 curves.

340

341

342

343

344

345

346   **References**

347   Batt, R. D., and S. R. Carpenter. 2012. Free-water lake metabolism: addressing noisy

348   time series with a Kalman filter. Limnol. Oceanogr. Methods **10**: 20-30.

349   Brothers, S. M., S. Hilt, K. Attermeyer, and others. 2013a. A regime shift from

350   macrophyte to phytoplankton dominance enhances carbon burial in a shallow,

351   eutrophic lake. Ecosphere **4**: 137.

352   Brothers, S. M., S. Hilt, S. Meyer, and J. Köhler. 2013b. Plant community structure

353   determines primary productivity in shallow, eutrophic lakes. Freshwater Biol. **58**:

354   2264-2276.

355   Caraco, N. F., and J. J. Cole. 2002. Contrasting impacts of a native and alien macrophyte

356   on dissolved oxygen in a large river. Ecol. Appl. **12**: 1496-1509.

357   Coloso, J. J., J. J. Cole, P. C. Hanson, and M. L. Pace. 2008. Depth-integrated,

358   continuous estimates of metabolism in a clear-water lake. Can. J. Fish. Aquat. Sci.

359   **65**: 712-722.

360   Coloso, J. J., J. J. Cole, and M. L. Pace. 2011. Short-term variation in thermal

361   stratification complicates estimation of lake metabolism. Aquat. Sci. **73**: 305-315.

362   Cremona, F., A. Laas, P. Nõges, and T. Nõges. 2014. High-frequency data within a

363   modeling framework: On the benefit of assessing uncertainties of lake metabolism.

364   Ecol. Mod. **294**: 27-35.

365   del Giorgio, P. A., and R. H. Peters. 1993. Balance between phytoplankton production

366   and plankton respiration in lakes. Can. J. Fish. Aquat. Sci. **50**: 282-289.

367   Downing, J. A., Y. T. Prairie, J. J. Cole, and others. 2006. The global abundance and size

368   distribution of lakes, ponds, and impoundments. Limnol. Oceanogr. **51**: 2388-2397.

369   Forrest, A. L., B. E. Laval, R. Pieters, and D. S. S. Lim. 2008. Convectively driven

370   transport in temperate lakes. Limnol. Oceanogr. **53**: 2321–2332.

371   Gelda, R. K., and S. W. Effler. 2002. Estimating oxygen exchange across the air-water

372   interface of a hypereutrophic lake. Hydrobiologia **487**: 243-254.

373   Hanson, P. C., S. R. Carpenter, N. Kimura, C. Wu, S. P. Cornelius, and T. K. Kratz.

374   2008. Evaluation of metabolism models for free-water dissolved oxygen methods in

375   lakes. Limnol. Oceanogr. Methods **6**: 454-465.

376   Hoellein, T. J., D. A. Bruesewitz, and D. C. Richardson. 2013. Revisiting Odum (1956):

377   A synthesis of aquatic ecosystem metabolism. Limnol. Oceanogr. **58**: 2089–2100.

378   Horsch, G. M., and H. G. Stefan. 1988. Convective circulation in littoral waters due to

379   cooling. Limnol. Oceanogr. **33**: 1068-1083.

380   Idrizaj, A., A. Laas, U. Anijalg and P. Nõges 2016. Horizontal differences in ecosystem

381   metabolism of a large shallow lake. J. Hydrol. **535**: 93-100.

382   James, W. F., and J. W. Barko. 1991. Littoral-pelagic phosphorus dynamics during

383   nighttime convective circulation. Limnol. Oceanogr. **36**: 949-960.

384   Lauster, G. H., P. C. Hanson., and T. K. Kratz. 2006. Gross primary production and

385   respiration differences among littoral and pelagic habitats in northern Wisconsin

386   lakes. Can. J. Fish. Aquat. Sci. **63**: 1130-1141.

387   MacIntyre, S., and J. M. Melack. 1995. Vertical and horizontal transport in lakes: linking

388   littoral, benthic, and pelagic habitats. J. N. Am. Benthol. Soc. **14**: 599-615.

389   McNair, J. N., L. C. Gereaux, A. D. Weinke, M. R. Sesselmann, S. T. Kendall, and B. A.

390   Biddanda. 2013. New methods for estimating components of lake metabolism based

391   on free-water dissolved-oxygen dynamics. Ecol. Mod. **263**: 251-263.

392   Monismith, S. G., J. Imberger, and M. L. Morison. 1990. Convective motions in the

393   sidearm of a small reservoir. Limnol. Oceanogr. **35**: 1676-1702.

394   Obrador, B., P. A. Staehr, and J. P. C. Christensen. 2014. Vertical patterns of metabolism

395   in three contrasting stratified lakes. Limnol. Oceanogr. **59**: 1228-1240.

396   Odum, H. T. 1956. Primary production in flowing waters. Limnol. Oceanogr. **1**: 102-117.

397   Oldham, C. E., and J. J. Sturman. 2001. The effect of emergent vegetation on convective

398   flushing in shallow wetlands: Scaling and experiments. Limnol. Oceanogr. **46**:

399   1486-1493.

400   Rose, K. C., L. A. Winslow, J. S. Read, E. K. Read, C. T. Solomon, R. Adrian, and P. C.

401   Hanson. 2014. Improving the precision of lake ecosystem metabolism estimates by

402   identifying predictors of model uncertainty. Limnol. Oceanogr.: Methods 12: 303-

403   312.

404   Sadro, S., J. M. Melack, and S. MacIntyre. 2011. Spatial and temporal variability in the

405   ecosystem metabolism of a high-elevation lake: integrating benthic and pelagic

406   habitats. Ecosystems. **14**: 1123-1140.

407   Salonen, K., M. Pulkkanen, P. Salmi, and R. W. Griffiths. 2014. Interannual variability of

408   circulation under spring ice in a boreal lake. Limnol. Oceanogr. **59**: 2121-2132.

409   Shatwell, T., A. Nicklisch, and J. Köhler. 2012. Temperature and photoperiod effects of

410   phytoplankton growing under simulated mixed layer light fluctuations. Limnol.

411   Oceanogr. **57**: 541-553.

412   Solomon, C. T., D. A. Bruesewitz, D. C. Richardson, and others. 2013. Ecosystem

413   respiration: drivers of daily variability and background respiration in lakes around

414   the globe. Limnol. Oceanogr. **58**: 849-866.

415   Staehr, P. A., D. Bade, M. C. Van de Bogert, and others. 2010. Lake metabolism and the

416   diel oxygen technique: State of the science. Limnol. Oceanogr.: Methods **8**: 628-

417   644.

418   Staehr, P. A., J. P. A. Christensen, R. D. Batt, and J. S. Read. 2012. Ecosystem

419   metabolism in a stratified lake. Limnol. Oceanogr. **57**: 1317-1330.

420   Sturman, J. J., C. E. Oldham, and G. N. Ivey. 1999. Steady convective exchange flows

421   down slopes. Aquat. Sci. **61**: 260-278.

422   They, N. H., D. da M. Marques, and R. S. Souza. 2013. Lower respiration in the littoral

423   zone of a subtropical shallow lake. Front. Microbiol. **3**: 434.

424   Tranvik, L., J. A. Downing, J. B. Cotner, and others. 2009. Lakes and impoundments as

425   regulators of carbon cycling and climate. Limnol. Oceanogr. **54**: 2298-2314.

426   Unmuth, J. M. L., R. A. Lillie, D. S. Dreikosen, and D. W. Marshall. 2000. Influence of

427   dense growth of Eurasian Watermilfoil on lake water temperature and dissolved

428   oxygen. J. Freshwater Ecol. **15**: 497-503.

429   Van de Bogert, M. C., S. R. Carpenter, J. J. Cole, and M. L. Pace. 2007. Assessing

430   pelagic and benthic metabolism using free water measurements. Limnol. Oceanogr.:

431   Methods **5**: 145-155.

432   Van de Bogert, M. C., D. L. Bade, S. R. Carpenter, J. J. Cole, M. L. Pace, P. C. Hanson,

433   and O. C. Langman. 2012. Spatial heterogeneity strongly affects estimates of

434   ecosystem metabolism in two north temperate lakes. Limnol. Oceanogr. **57**: 1689-

435   1700.

436   Verpoorter, C., T. Kutser, D. A. Seekell, and L. J. Tranvik. 2014. A global inventory of

437   lakes based on high-resolution satellite imagery. Geophys. Res. Lett. **41**: 6396–

438   6402.

439   Winslow, L. A., J. A. Zwart, R. D. Batt, H. A. Dugan, R. I. Woolway, J. R. Corman, and

440   J. S. Read. 2016. LakeMetabolizer: an R package for estimating lake metabolism

441   from free-water oxygen using diverse statistical methods. Inland Waters **6**: 622-636.

442

443

444

445

446

447

448

449

450

451

452

453

454

455

456

457

458

468

469

470

471

472

473

474

475

476

477

478

479

480

481

482 **Table 1.** Seasonality of calculated gross primary production (GPP) and related

483 meteorological data (May 8th, 2010 to May 7th, 2011).

	Percentage of negative GPP values	Mean whole-lake GPP from diel-O_2 curves, negatives included (g C m^{-2} y^{-1})	Mean whole-lake GPP from diel-O_2 curves, negatives excluded (g C m^{-2}y^{-1})	Phytoplankton GPP from P-I curves (g C m^{-2}y^{-1})	Mean wind speed (m s^{-1})	Mean day-to-night air temp. diff. (°C)
Spring (Mar-May)	30	138 ± 49 (*n* = 54)	307 ± 44 (*n* = 38)	165 ± 7 (n = 55)	1.26 ± 0.05	6.4 ± 0.6 (*n* =24)
Summer (Jun-Aug)	40	99 ± 52 (*n* = 88)	422 ± 41 (*n* = 53)	476 ± 17 (*n* = 88)	1.08 ± 0.04	9.2 ± 0.4 (*n* = 88)
Fall (Sep-Nov)	32	119 ± 26 (*n* = 86)	232 ± 27 (*n* = 58)	142 ± 6 (*n* = 86)	1.14 ± 0.04	5.6 ± 0.4 (*n* =

						86)
Winter (Dec-Feb)	81	-33 ± 25 (*n* = 63)	263 ± 99 (*n* = 11)	0 (n = 64)*	NA	3.9 ± 0.4 (*n* =65)
Total	45	83 ± 21 (*n* = 291)	315 ± 22 (*n* = 160)	216 ± 12 (*n* = 293)	0.90 ± .03	6.5 ± 0.2 (*n* = 263)

484   * Due to snow and ice cover, with resulting light transmittance anticipated to be low,

485   wintertime phytoplankton GPP was estimated to be zero.

486

487

488

489

490

491

492

493

494

495

496

497

Figure captions

499

500　**Figure 1.** Convective flow of oxygen from littoral to pelagic lake zones (black arrows)

501　above and parallel to the thermocline (dashed line) due to differential heating during the

502　day and differential cooling at night (adapted from Monismith et al. (1990) and Oldham

503　and Sturman (2001)). When coupled with higher primary production in the littoral zone

504　during the day and higher respiration at night, this convective flow may explain

505　unexpected oxygen curves measured at a central probe (such as rising overnight oxygen

506　concentrations).

507

508　**Figure 2.** Theoretical diel oxygen curves, showing higher primary productivity in the

509　littoral zone than the pelagic zone, and the resulting offset under advective current

510　conditions.

511

512　**Figure 3.** Sample oxygen measurements from Schulzensee (black circles), showing the

513　volumetric primary productivity rates (represented by the slopes of the solid and dashed

514　lines) which would result from the measured oxygen curves (solid lines, below measured

515　oxygen points), compared to independently determined phytoplankton production for the

516　same days (dashed lines, above oxygen points). Grey zones represent nighttime periods.

517

518　**Figure 4.** Full-year gross primary production of Schulzensee, as calculated from diel O_2

519　curves by LakeMetabolizer, comparing Bayesian, Kalman, bookkeeping, maximum-

520　likelihood estimation (MLE), and ordinary least squares (OLS) approaches. Boxes

24

521   represent the upper quartile, median, and lower quartile of values, with whiskers

522   representing the 5th and 95th percentiles. Centered squares represent the mean value, and

523   crosses designate minimum and maximum values in the dataset.

524

525

526
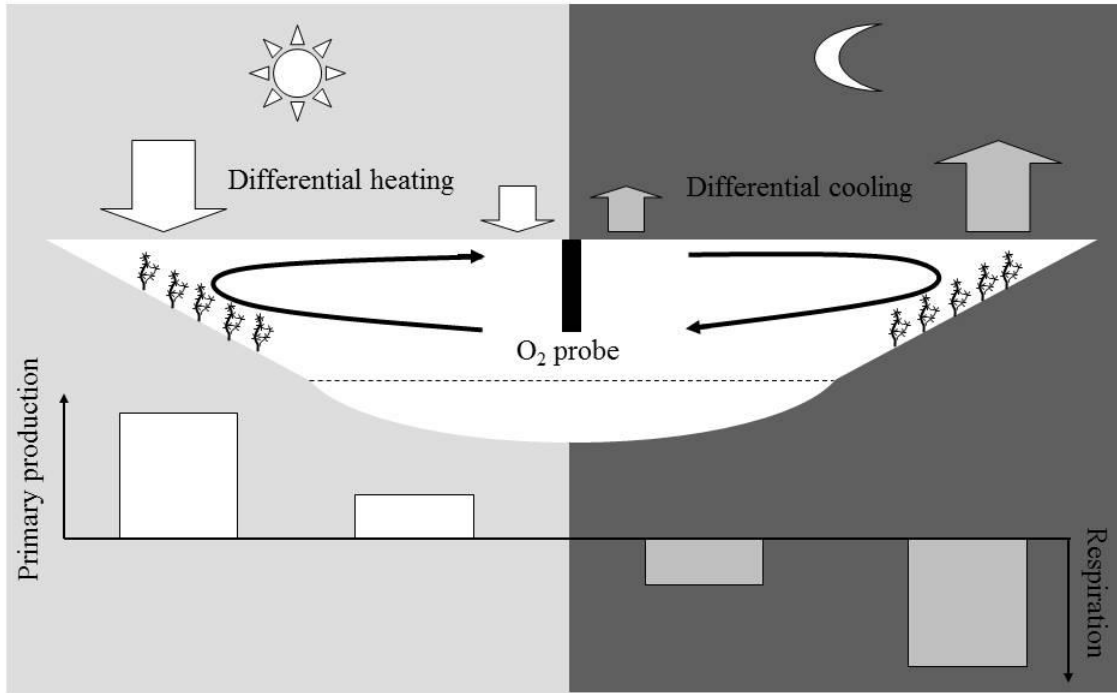
527

528

529

530

531

532

533

534

535

536

537

538

539

540

541

542

543

544
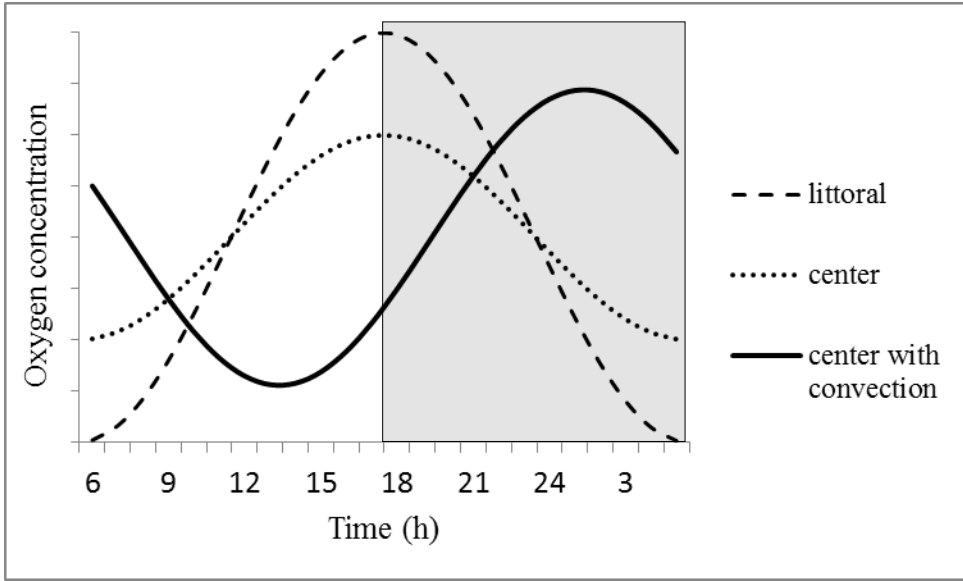
545   Fig. 1

546

547

548

549

550

551

552

553

554

555

556

557

558

559　Fig 2.

560

561

562

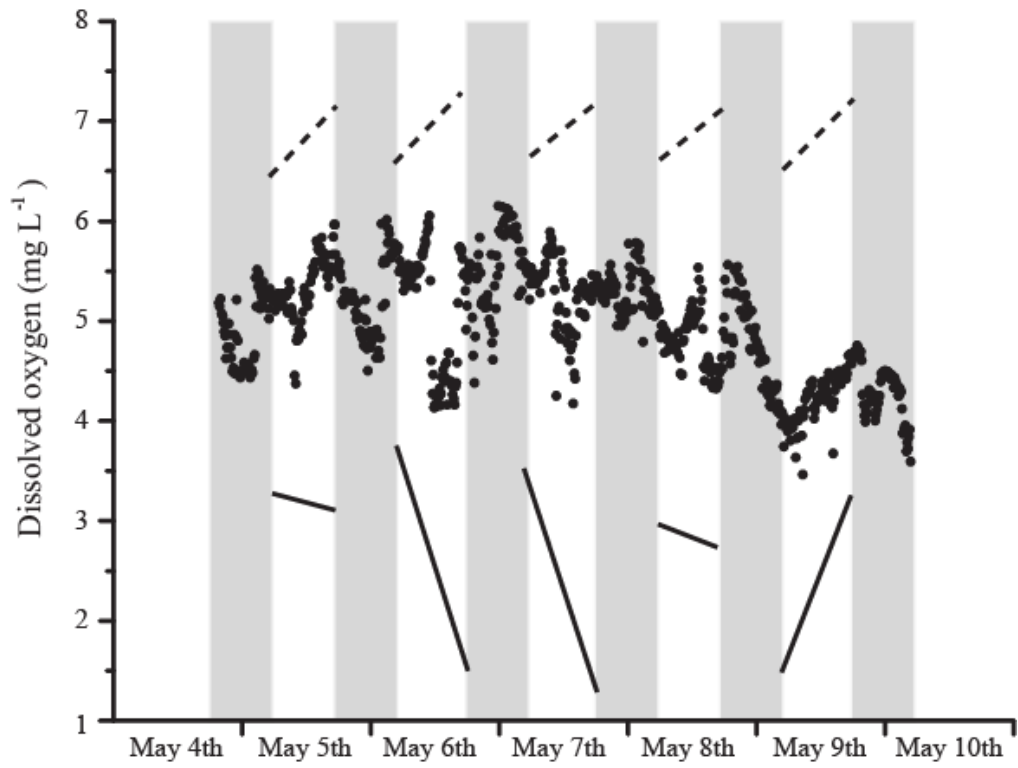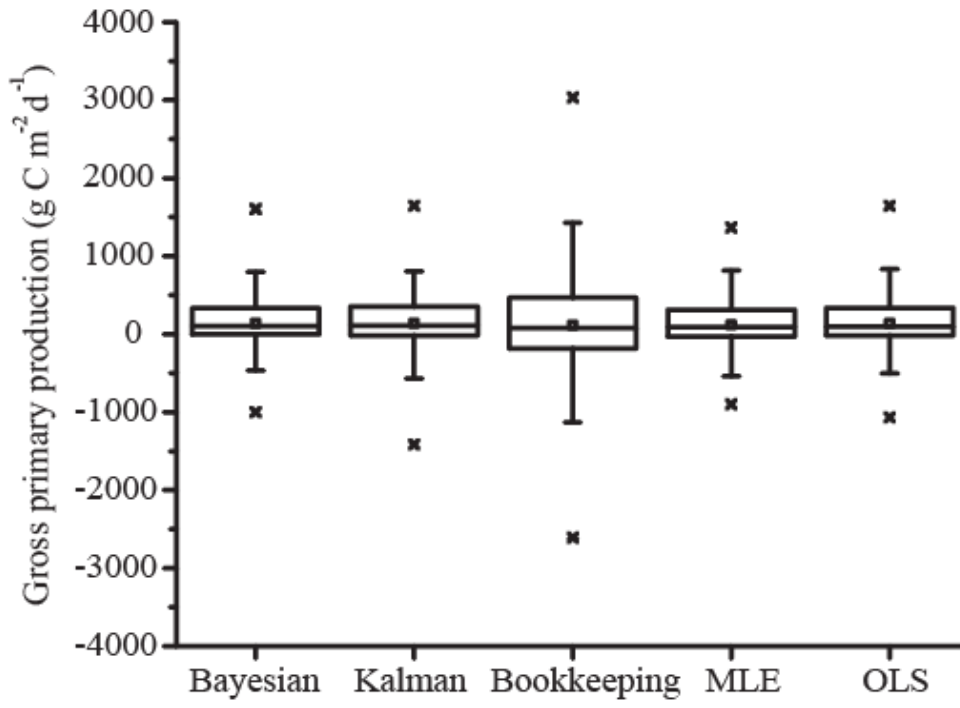563

564

565

566

567

568

569

570

571   Fig. 3

572

573

574

575

576

577

578

579

580

581

582

583

584

585   Fig. 4